Quasi-Z-Source-Based Isolated DC/DC Converters for Distributed Power Generation

Dmitri Vinnikov, *Member, IEEE*, and Indrek Roasto

Abstract—This paper presents new step-up dc/dc converter topologies intended for distributed power generation systems. The topologies contain a voltage-fed quasi-Z-source inverter with continuous input current on the primary side, a single-phase isolation transformer, and a voltage doubler rectifier (VDR). To increase the power density of the converter, a three-phase auxiliary ac link (a three-phase inverter and a three-phase isolation transformer) and a three-phase VDR are proposed to be implemented. This paper describes the operation principles of the proposed topologies and analyzes the theoretical and experimental results.

Index Terms—DC–DC power conversion, fuel cells (FCs), pulsewidth-modulated power converters, rectifiers.

I. INTRODUCTION

DISTRIBUTED power generation, when fully implemented, can provide reliable, high-quality, and low-cost electric power. As a modular electric power generation close to the end user, it offers savings in the cost of grid expansion and line losses. If connected to the power grid, the bidirectional transactions between the grid and the local generation result in grid capacity enhancement, virtually uninterrupted power supply, and optimum energy cost due to the availability of use/purchase/sales options [1].

Distributed power is a concept that covers a wide spectrum of schemes used for local electric power generation from renewable and nonrenewable sources of energy in an environmentally responsible way. Basic schemes are mainly based on solar energy, wind energy, fuel cells (FCs), and microturbines.

An FC is potentially the most efficient modern approach to distributed power generation. The efficiency of the conversion, i.e., the ratio of the electrical output to the heat content of the fuel, could be as high as 65%–70% [1]. In fact, its electrical efficiency could be greater than 70% in theory. Current technologies have only been capable of reaching efficiencies of around 45%. Combined cycles are intended to raise electrical efficiency up to 60% for plants based on high-temperature cells [2].

To interconnect a low-dc-voltage-producing FC (typically 40–80 Vdc) to residential loads (typically 230-Vac single phase or 3 × 400 Vac), a special voltage matching converter is required. A typical structure of a two-stage interface converter is shown in Fig. 1. Due to safety and dynamic performance

requirements, the interface converter should be realized within the dc/dc/ac concept. This means that low voltage from the FC first passes through the front-end step-up dc/dc converter with the galvanic isolation; subsequently, the output dc voltage is inverted in the three-phase inverter and filtered to comply with the imposed standards and requirements (second dc/ac stage).

The design of the front-end isolated dc/dc converter is most challenging because this stage is the main contributor of interface converter efficiency, weight, and overall dimensions. The low voltage provided by the FC is always associated with high currents in the primary part of the dc/dc converter (switching transistors and primary winding of the isolation transformer). These high currents lead to high conduction and switching losses in the semiconductors and therefore reduce the efficiency. Moreover, the large voltage boost factor requirement presents a unique challenge to the dc/dc converter design [2]. This specific requirement could be fulfilled in different ways: by use of an auxiliary boost converter before the isolated dc/dc converter [3]–[7] or by use of an isolation transformer with a large turns ratio [8]–[14] for effective voltage step-up.

In the first case [Fig. 2(a)], the auxiliary boost converter steps up the varying FC voltage to a certain constant voltage level (80–100 Vdc) and supplies the input terminals of the isolated dc/dc converter. In that case, the primary inverter within the dc/dc converter operates with a near-constant duty cycle, thus ensuring better utilization of an isolation transformer. Moreover, due to preboosted input voltage, the isolation transformer has the moderate turns ratio (1:7–1:8), which exerts a positive impact in terms of leakage inductance and efficiency. A very interesting solution is proposed in [5], where the conventional inductor in an auxiliary boost converter is replaced with a zero-ripple filter (ZRF). The ZRF comprises a coupled inductor-based filter for minimizing the high-frequency switching ripple and an active power filter for mitigating the low-frequency ripple. Despite evident advantages of the isolated dc/dc converter with an auxiliary boost converter, its main drawbacks are drawn from the multistage energy conversion structure, i.e., complicated control and protection algorithms and reduced reliability due to the increased number of switching devices.

A direct step-up dc/dc converter without input voltage preregulation [Fig. 2(b)] is simpler in control and protection. Due to the reduced number of switching devices, the converter tends to have better efficiency and reliability. The varying voltage from the FC passes through the high-frequency inverter to the step-up isolation transformer. The magnitude of the primary winding voltage is controlled by the duty cycle variation of inverter switches in accordance with the FC output voltage and converter load conditions. The isolation transformer should
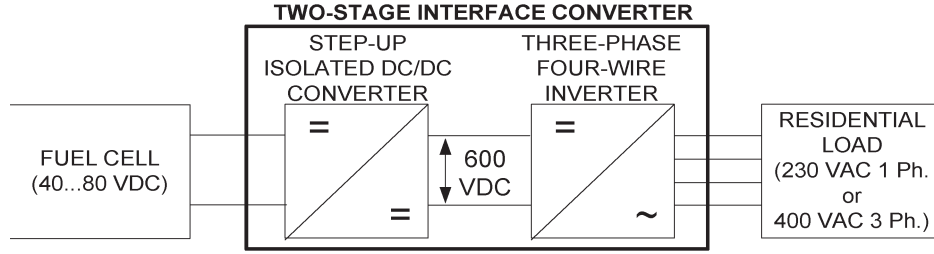
TWO-STAGE INTERFACE CONVERTER

Fig. 1. Typical structure of the interface converter for residential FC-powered systems.
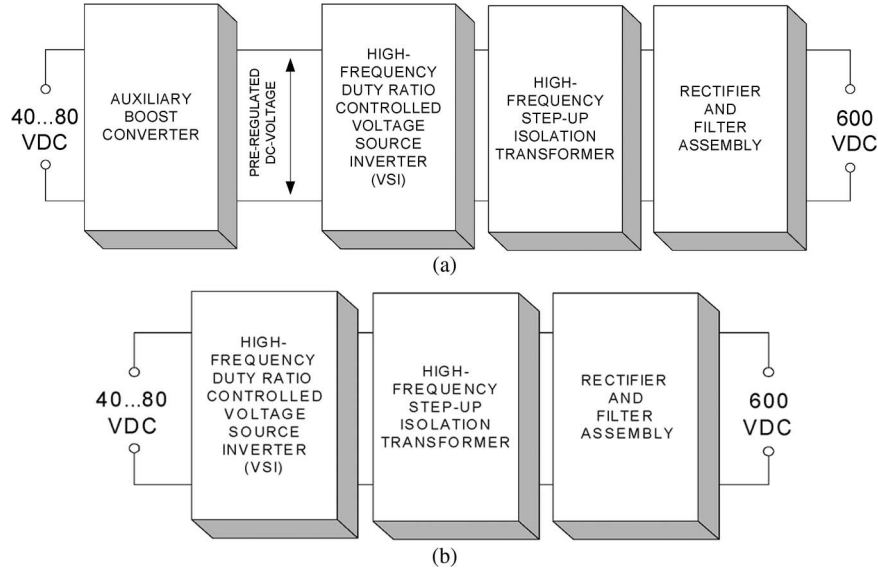
Fig. 2. Generalized structures of most widespread front-end step-up isolated dc/dc converters for residential FC power systems.

have an increased turns ratio (approximately $1:17$) to provide effective voltage step-up in the whole range of input voltage and load variations. The choice of dc/dc converter topology in that case can be broadly categorized as a push–pull or a single-phase full-bridge topology. Because of the symmetrical transformer flux and minimized stress of primary inverter switches, the full-bridge topology has been found to be most useful in terms of cost and efficiency, particularly when implemented for power levels higher than 3 kW [8].

This paper is devoted to a new power circuit topology to be implemented in the front-end dc/dc converter for distributed power generation. The topology proposed (Fig. 3) contains a voltage-fed quasi-Z-source inverter (qZSI) with continuous input current at the converter input side, a high-frequency step-up isolation transformer, and a voltage doubler rectifier (VDR). In contrast to earlier presented topologies [3]–[14], the novel converter provides such advantages as increased reliability, isolation transformer with reduced turns ratio, and reduced impact on the FC due to continuous input current. To improve the power density of the converter, the topology with a three-phase intermediate ac link is discussed in the final section of this paper.

II. DESCRIPTION OF PROPOSED TOPOLOGY

The voltage-fed qZSI with continuous input current implemented at the converter input side (Fig. 3) has a unique feature:

It can boost the input voltage by utilizing extra switching state—the shoot-through state. The shoot-though state here is the simultaneous conduction of both switches of the same phase leg of the inverter. This operation state is forbidden for the traditional voltage source inverter (VSI) because it causes the short circuit of the dc-link capacitors. In the discussed qZSI, the shoot-through state is used to boost the magnetic energy stored in the dc-side inductors ($L1$ and $L2$ in Fig. 3) without short-circuiting the dc capacitors. This increase in inductive energy, in turn, provides the boost of voltage seen on the transformer primary winding during the traditional operating states (active states) of the inverter. Thus, the varying output voltage of the FC is first preregulated by adjusting the shoot-through duty cycle; afterward, the isolation transformer is being supplied with a voltage of constant amplitude value. Although the control principle of the qZSI is more complicated than that of a traditional VSI, it provides a potentially cheaper, more powerful, reliable, and efficient approach to be used for FC-powered systems.

The voltage-fed qZSI with continuous input current was first presented in [15] as a modification of a currently popular voltage-fed Z-source inverter (ZSI) [16]–[18]. The drawback associated with the conventional ZSI is substantial—discontinuous input current during the boost mode that could have a negative influence on the FC. The discussed qZSI shown in Fig. 3 features continuous current drawn from the FC as well as lower operating voltage of the
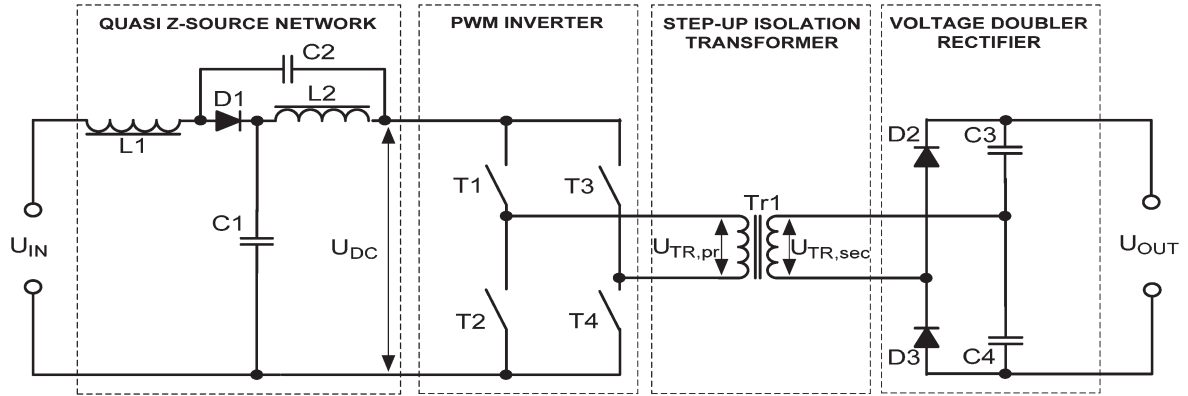
Fig. 3.   Simplified power circuit diagram of the proposed converter.

capacitor $C2$, as compared to the ZSI topology. The operating dc voltages of the capacitors $C1$ and $C2$ could be estimated as

$$U_{C1} = \frac{1 - D_S}{1 - 2D_S} \cdot U_{IN} \tag{1}$$

$$U_{C2} = \frac{D_S}{1 - 2D_S} \cdot U_{IN} \tag{2}$$

where D_S is the duty cycle of the shoot-through state

$$D_S = \frac{t_S}{T} \tag{3}$$

where t_S is the duration of the shoot-through state and T is the operation period.

When the input voltage is high enough, the shoot-through states are eliminated, and the qZSI starts to operate as a traditional VSI, thus performing only the buck function of the input voltage. Thus, the qZSI could realize both the voltage boost and the buck functions without any additional switches using a special control algorithm only.

A. Voltage Boost Control Method of qZSI-Based Single-Phase DC/DC Converter

Fig. 4 shows the control principle of the single-phase qZSI in the shoot-through (voltage boost) operating mode. Fig. 4(a) shows the switching pattern of the traditional single-phase VSI. These switching states are known as active states when one and only one switch in each phase leg conducts. To generate the shoot-through states, two reference signals (U_p and U_n) were introduced [Fig. 4(b)]. If the triangle waveform is greater than U_p or lower than U_n, the inverter switches turn into the shoot-through state [Fig. 4(b)]. During this operating mode, the current through the inverter switches reaches its maximum. Depending on the control algorithm, the shoot-through current could be distributed between one or both inverter legs. The dc-link voltage and the primary winding voltage waveforms of the isolation transformer during shoot-through are shown in Fig. 4(c) and (d), respectively.

According to the presented control methodology (Fig. 4), the shoot-through states are created during the zero states of the full-bridge inverter, where the primary winding of the isolation transformer is shorted through either the top ($T1$ and $T3$) or
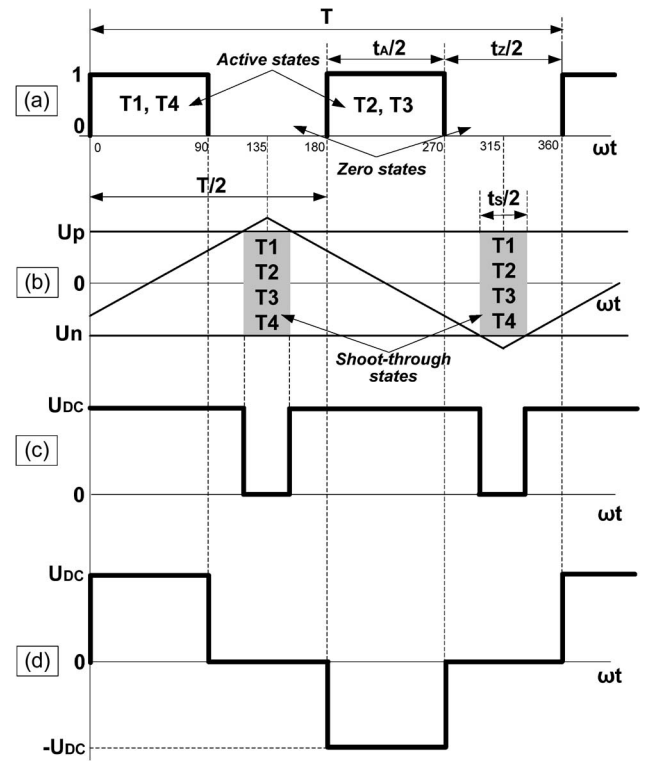

Fig. 4.   Proposed operating principle and resulting voltages of the single-phase qZSI in the shoot-through (voltage boost) mode.

bottom ($T2$ and $T4$) inverter switches. To provide a sufficient regulation margin, the zero-state time t_Z should always exceed the maximum duration of the shoot-through states $t_{S,\max}$ per one switching period

$$t_Z > t_{S,\max}. \tag{4}$$

Thus, each operating period of the qZSI during the shoot-through always consists of an active state t_A, shoot-through state t_S, and zero state t_Z

$$T = t_A + t_S + t_Z. \tag{5}$$

Equation (5) could also be represented as

$$\frac{t_A}{T} + \frac{t_S}{T} + \frac{t_Z}{T} = D_A + D_S + D_Z = 1 \tag{6}$$

TABLE I
DESIRED OPERATING PARAMETERS OF INVESTIGATED CONVERTER

Parameter	Value
Minimal input voltage, $U_{IN,min}$	40 V
Maximal input voltage, $U_{IN,max}$	80 V
Desired DC-link voltage amplitude, U_{DC}	80 V
Desired output voltage of the converter, U_{OUT}	600 V
Operating frequency of the isolation transformer, f_{TR}	5 kHz
Operating frequency of the qZS-network, f	10 kHz
Desired voltage ripple of the capacitors	$\leq 1\%$
Desired peak-to-peak current ripple through the inductors	$\leq 20\%$

where D_A is the duty cycle of an active state, D_S is the duty cycle of a shoot-through state, and D_Z is the duty cycle of a zero state. It should be noted that the duty cycle of the shoot-through state must never exceed 0.5. It should be noted here that, in the presented control scheme, the shoot-through time interval is evenly split into two intervals of half the duration. In that case, the operating frequency of the quasi-Z-source (qZS) network will be two times higher, and the resulting switching frequency of the power transistors will be up to three times higher [Fig. 8(a)] than the fundamental harmonic frequency of the isolation transformer. That fact is very relevant for proper component and operating frequency selection.

In the operating points, when the input voltage is high enough, the shoot-through states are eliminated, and the qZSI operates as a traditional VSI. Thus, the qZSI discussed could provide both the voltage boost and buck functions by the single-stage energy conversion.

B. Power Circuit Design Considerations

This section provides an overview of the design process of the proposed dc/dc converter. The desired operating parameters are presented in Table I.

In the given application, the desired value selected for the dc-link voltage U_{DC} was 80 V. It is assumed that the converter is always operating with the rated load and between two boundary operating points, which correspond to the minimal $U_{IN,min}$ and maximal $U_{IN,max}$ input voltages. In the first case, the shoot-through states should be used to boost the input voltage to the predefined dc-link voltage level. In the second case, when the input voltage is equal to the desired dc-link voltage, no shoot-through is applied, and the qZSI operates as a traditional VSI.

The design of the power converter should be performed for the operating point with a minimal possible input voltage and at rated power, when the shoot-through duty cycle reaches its maximum. As a consequence, the boost ratio of the input voltage is also maximal

$$B_{\max} = \frac{U_{DC}}{U_{IN,\min}} = \frac{80}{40} = 2. \qquad (7)$$

To achieve proper efficiency of the converter and better transformer utilization, in real designs, proper balance between the boost ratio and the transformer turns ratio should be found.

In the current application, the maximal duty cycle of the shoot-through state is

$$D_{S,\max} = \frac{1 - (B_{\max})^{-1}}{2} = 0.25. \qquad (8)$$

During the active states, the transformer primary winding is being supplied from the inverter by a voltage with an amplitude value $U_{TR,pr} = U_{DC} = 80$ V. To reduce the turns ratio n of the isolation transformer, a VDR was implemented on the secondary side of the converter. In contrast to the traditional full-bridge rectifier, two diodes of one leg in the VDR topology are replaced by the capacitors. Since each capacitor charges to the peak secondary voltage $U_{TR,sec}$, the output voltage from this circuit will be the sum of the two capacitor voltages or twice the peak voltage of the secondary winding. This circuit then produces an output voltage that is twice the transformer secondary voltage. Due to the voltage doubling effect, the VDR enables the use of the isolation transformer with a reduced secondary turns ratio, i.e., $1 : 3.75$ for the application discussed. Furthermore, the VDR improves the rectification efficiency due to minimized voltage drops in the components (twice reduced number of rectifying diodes and full elimination of a smoothing inductor).

For every operating point within the predefined boundaries $[U_{IN,min}; U_{IN,max}]$, the output voltage of the converter could be estimated as

$$U_{OUT} = \frac{2 \cdot U_{IN} \cdot B}{n} = \frac{2 \cdot U_{IN}}{n} \cdot \left(\frac{1}{1 - 2 \cdot D_S} \right) \qquad (9)$$

where n is the turns ratio of the isolation transformer. To limit the voltage ripple on the output half-bridge capacitors ($C3$ and $C4$), e.g., by 1% (6 V) at peak power P, the capacitance should be

$$C3 = C4 = \frac{P \cdot (1 - D_A)}{0.01 \cdot f_{TR} \cdot (U_{OUT})^2}. \qquad (10)$$

Inductors and capacitors of the qZS network should also be selected in compliance with the desired current and voltage ripples on the elements during the shoot-through and active states. The design guidelines are described in detail in [19] and [20].

III. COMPUTER SIMULATIONS OF PROPOSED CONVERTER

The assumptions presented earlier were verified by computer simulations in both operating points $U_{IN,min}$ and $U_{IN,max}$ and at rated load. To control the power transistors in the qZSI, a special gating signal generation circuit was developed (Fig. 5). The active and zero states are generated by two 180° phase-shifted pulsewidth-modulated generators and by two NOT logic gates. The shoot-through states are generated using a triangle waveform generator and two comparators. When the modulation waveform is greater than the value of the reference signal U_p, the first shoot-through state (all the transistors turned on) appears, and when the modulation signal is smaller than the reference signal U_n, the second shoot-through state emerges.
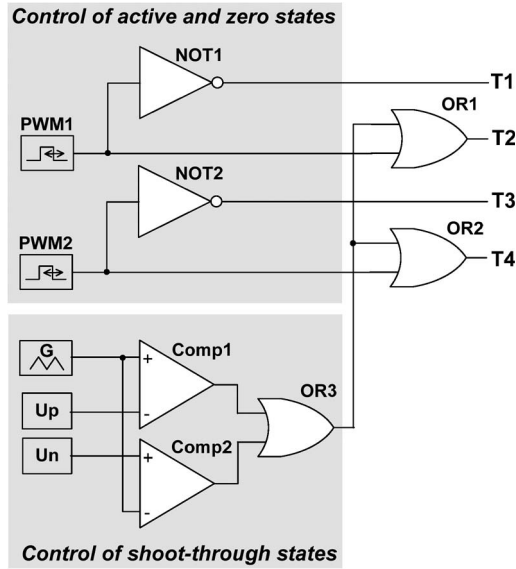
Fig. 5. Generalized block diagram of a gating signal generator.

Fig. 6. Simulation results of the proposed converter during the minimal input voltage and maximal shoot-through duty cycle ($D_S = 0.25$). (a) Gating signals of transistors ($T1-T4$) and resulting primary voltage of the isolation transformer ($U_{\mathrm{TR,pr}}$). (b) Input (U_{IN}), dc-link (U_{DC}), primary winding ($U_{\mathrm{TR,pr}}$), secondary winding ($U_{\mathrm{TR,sec}}$), and output (U_{OUT}) voltage waveforms.

The simulation software specifically designed for power electronics and motor control simulation model of the proposed converter was developed in accordance with schematics shown in Fig. 3. The following system parameters were assumed for the converter during simulations: $P = 500$ W, $C1 = C2 = 240$ μF, $L1 = L2 = 50$ μH, and $C3 = C4 = 10$ μF. The isolation transformer has the turns ratio of $1:3.75$. To demonstrate the basic operating waveforms, the converter was first studied in both boundary operating points, e.g., with minimal (40 V) and maximal (80 V) input voltages and at rated loads. Afterward, the transient response simulations were performed. The duty cycle of active states per switching period was set at $D_A = 0.5$ and remained unchanged for all simulations. The simulation results are shown in Figs. 6 and 7.

A. Basic Operating Waveforms of Converter

First simulations (Fig. 6) were performed with an input voltage $U_{\mathrm{IN,min}} = 40$ V and the maximal shoot-through duty cycle ($D_S = 0.25$ per switching period). To provide good visualization, simulation waveforms are presented with the timescale corresponding to one full period of the operating voltage of the isolation transformer. The operating frequency of the qZS network is twice the operating frequency of the isolation transformer. The zero states are produced by the simultaneous conduction of the top-side transistors ($T1$ and $T3$). Based on the control algorithm implemented, the switching frequency of the top-side transistors in the shoot-through mode is equal to the operating frequency of the isolation transformer, while the switching frequency of the bottom-side transistors ($T2$ and $T4$) is three times higher than that of $T1$ and $T3$. Fig. 6(b) shows that the qZSI with the proposed control algorithm ensures the demanded gain of the input voltage ($U_{\mathrm{IN}} = 40$ V and $U_{\mathrm{DC}} = 80$ V, as expected). Moreover, the VDR provides the demanded voltage doubling effect of the peak voltage of the secondary winding of the isolation transformer, thus ensuring the ripple-free output voltage of 600 Vdc at the rated power.
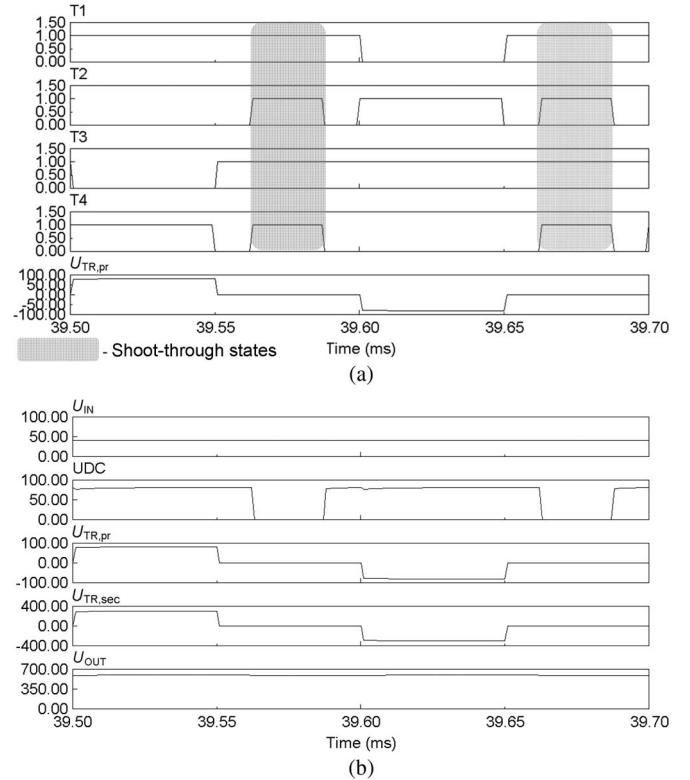
For the second operating point (Fig. 7), when the input voltage equals the desired dc-link voltage, the shoot-through states are eliminated, and the converter operates as a traditional VSI. The operating frequency of the top- and bottom-side transistors is the same in that case, and it equals that of the isolation transformer.

B. Stability Margin and Compensation Loop Design

Since the proposed converter topology is a higher order system, the stability criteria and the design of the control loop are important issues. A good method to test system stability and dynamic behavior is transient response analysis. In the case of combined regulation, i.e., when both the load and the input voltage are changing simultaneously, two transient tests should be carried out: input voltage and load transient response. It was assumed that the input voltage and the load are not changed simultaneously. In the case of input voltage transient response, the input voltage source works as a square-wave signal generator with an output voltage range of 40–70 V, the shoot-through duty cycle is fixed at 0.05, and the load is chosen such that, at maximal input voltage, maximal output power could be achieved. In order to obtain an open-loop load transient response, the input voltage is fixed at 80 V, the shoot-through duty cycle is set to zero, and the load is changed periodically between 100% and 50% of the maximal load. The simulation results of the input voltage and load transient response are shown in Fig. 8.
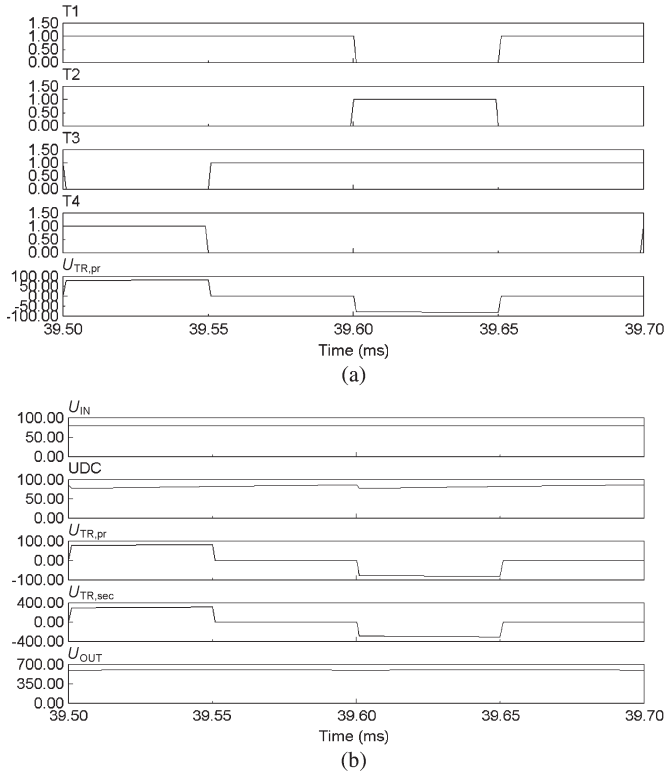
Fig. 7. Simulation results of the proposed converter during the maximal input voltage and "no-boost" mode ($D_S = 0$). (a) Gating signals of transistors ($T1-T4$) and resulting primary voltage of the isolation transformer ($U_{\mathrm{TR,pr}}$). (b) Input (U_{IN}), dc-link (U_{DC}), primary winding ($U_{\mathrm{TR,pr}}$), secondary winding ($U_{\mathrm{TR,sec}}$), and output (U_{OUT}) voltage waveforms.

Fig. 8. Simulation results of the (a) input voltage and (b) load transient response.

The output voltage waveform (U_{OUT}) in Fig. 8(a) shows a stable output with a good input damping; accordingly, a good closed-loop behavior could be assumed. During the load transient response simulations [Fig. 8(b)], the system shows excellent stability and fast response to load changes, which indicates an inherent stability of the proposed converter.

In order to regulate the output voltage, a gain compensator is needed. It is important to notice that, due to the voltage doubler, the output voltage does not depend on the active-state duty cycle. Therefore, the active-state duty cycle is kept constant at its maximum value. According to (9), the output voltage can be changed by the variation of the shoot-through duty cycle D_S. Taking into account all system parameters and operating conditions, like wide input voltage and load variation ranges, increased noise levels due to the shoot-through states, and no output inductor, the most optimal control algorithm seems to be the voltage mode control (VMC) [21], [22]. VMC is a single-loop control algorithm. The computer model of the control system is shown in Fig. 9. The output voltage is measured and compared with a setpoint. A type II compensation is used to stabilize the output voltage. The output of the regulator is scaled so that it can be directly used for the shoot-through duty cycle.

The simulations were carried out in combined regulation conditions. The input voltage was changed between 40 and 80 V, while the load was changed periodically between 50% and 100% of its maximal value. Type II compensation and the proposed control algorithm worked perfectly, as can be seen
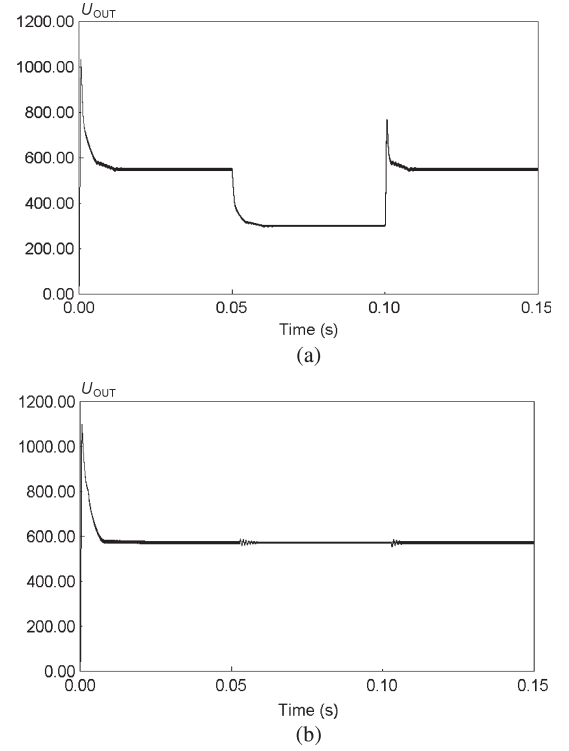
in Fig. 10. In the combined regulation conditions, stabilized nominal output voltage could be achieved.

IV. EXPERIMENTAL VERIFICATION OF THE PROPOSED CONVERTER

All the theoretical assumptions were verified on the experimental setup of the qZSI-based single-phase dc/dc converter. As the experiments show (Figs. 11–16), the simulated and measured results are in full agreement for both boundary operating points of the converter. Moreover, it was stated that the discussed topology ensures continuous input current during the voltage boost mode [Fig. 11(a)], thus reducing a negative impact on the proton exchange membrane of the FC module. The peak-to-peak current ripple could be further decreased by the implementation of inductors in the qZS network with increased inductance values.

Moreover, it was verified that the proposed VDR (two fast-recovery epitaxial diodes and two 10-μF film capacitors) coupled with a high-frequency isolation transformer (turns ratio of $1 : 3.75$) ensures effective voltage step-up with very compact size, extra low power dissipation, and with no remarkable ripple on the output voltage profile [Fig. 11(b)]. The operating waveforms of the isolation transformer (Fig. 13) of the proposed converter are very similar to those of a traditional isolated dc/dc converter with the VSI.

The second group of experiments (Figs. 14–16) was carried out at input voltage $U_{\mathrm{IN,max}} = 80$ V. In that operating point, the shoot-through mode was fully eliminated ($D_S = 0$), and the single-phase qZSI was operated as a traditional VSI without any modifications in hardware. As in the operating point at minimal
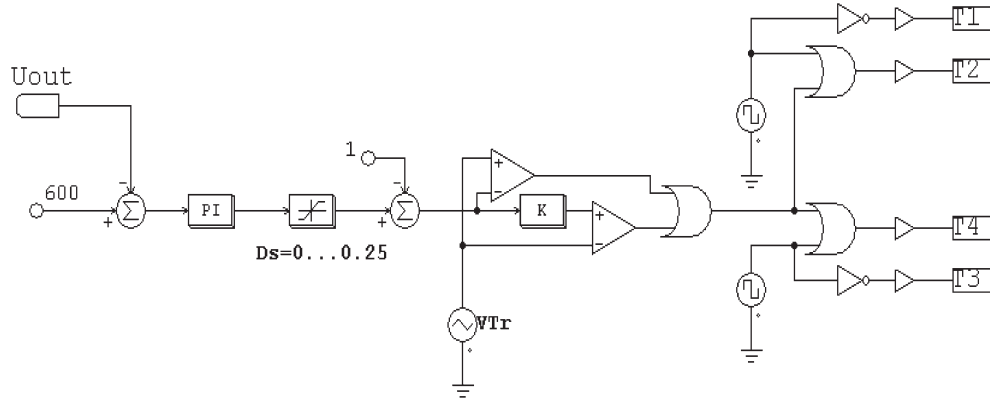
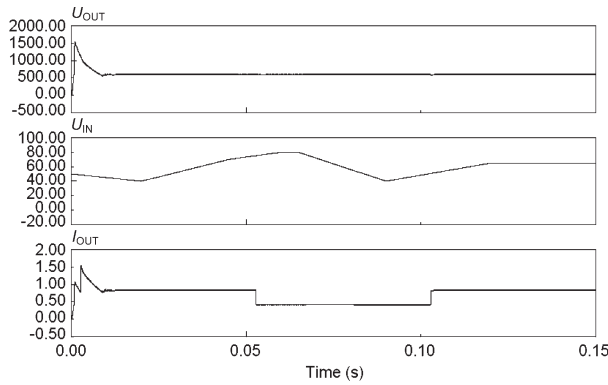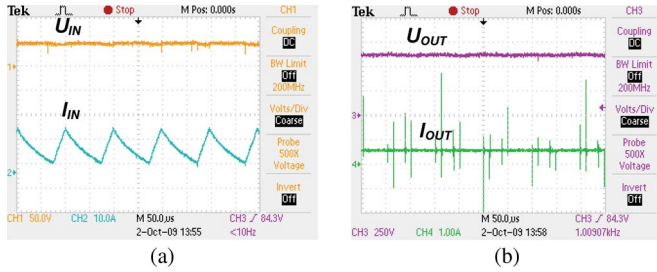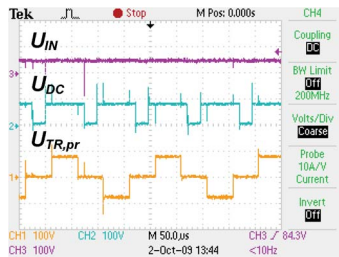Fig. 9.   VMC algorithm for the proposed converter.

Fig. 10.   Closed-loop response of the converter under pulse loading and changing input voltage conditions.

Fig. 11.   (a) Input and (b) output voltages and currents of the converter during the minimal input voltage and maximal shoot-through duty cycle ($D_S = 0.25$).

Fig. 12.   Operating voltage waveforms of the qZSI during the minimal input voltage and maximal shoot-through duty cycle ($D_S = 0.25$).

input voltage, the VDR ensures the demanded voltage doubling effect with no remarkable ripple on the output voltage profile [Fig. 14(b)].
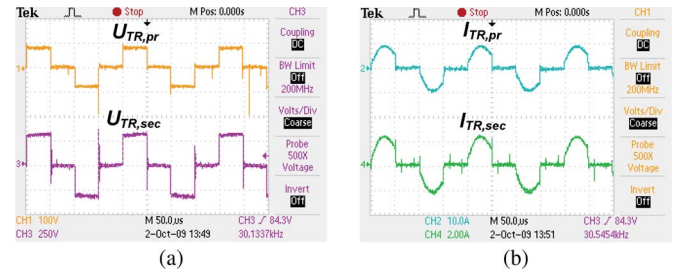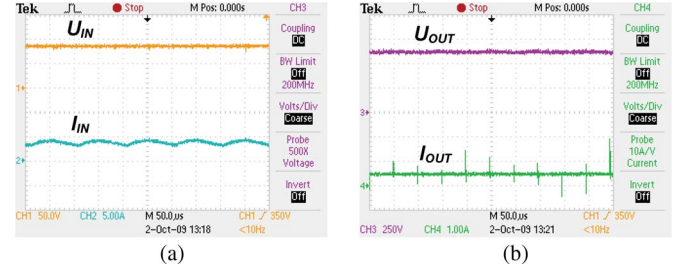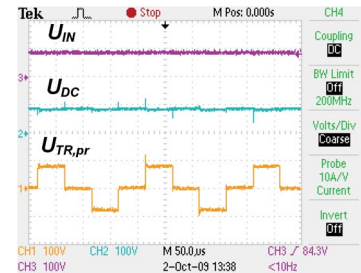

Fig. 13.   (a) Operating voltages and (b) currents of the high-frequency step-up isolation transformer during the minimal input voltage and maximal shoot-through duty cycle ($D_S = 0.25$).

Fig. 14.   (a) Input and (b) output voltages and currents of the converter during the maximal input voltage and "no-boost" mode ($D_S = 0$).

Fig. 15.   Operating voltage waveforms of the qZSI during the maximal input voltage and "no-boost" mode ($D_S = 0$).

Fig. 17 shows the efficiency of the new proposed converter obtained experimentally. The maximal efficiency (close to 95%) was obtained at the rated load (500 W) and maximal input voltage, where the shoot-through states are fully eliminated. At the minimal input voltage and rated load, when the shoot-through duty cycle becomes maximal, the efficiency drops to 85%. It was stated that the major power dissipation occurs in
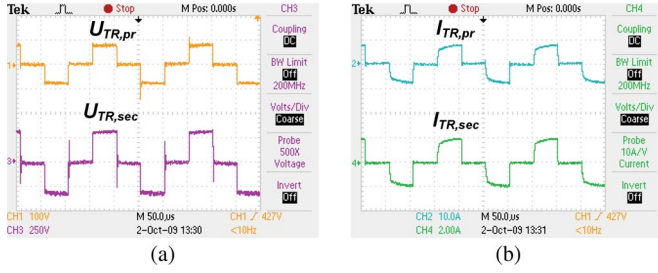
Fig. 16.   (a) Operating voltages and (b) currents of the high-frequency step-up isolation transformer during the maximal input voltage and "no-boost" mode ($D_S = 0$).
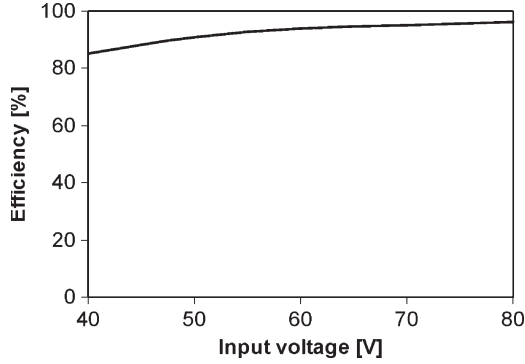

Fig. 17.   Measured efficiency versus input voltage for the rated power of the experimental converter.

inductors $L1$ and $L2$ of the qZS network. Inductors implemented in the prototype were not properly matching the design criteria. Operating with more than 80% peak-to-peak current ripple, they have increased hysteresis losses, thus affecting the overall efficiency of the converter.

V. qZSI-BASED DC/DC CONVERTER WITH THREE-PHASE INTERMEDIATE AC LINK AND VDR

Modern trends in residential power systems are directed to increased efficiency and power density of electronic converters to enhance the feasibility of the whole system. For the discussed application, an increase in power density (more power for the same volumetric space of the converter) could be achieved by the implementation of the three-phase intermediate ac link instead of the single-phase one. The hardware modifications are shown in Fig. 18. In contrast to the single-phase topology, the three-phase configuration has an additional inverter leg, two extra isolation transformers, and an additional rectifier diode leg. For every operating point within the predefined boundaries $[U_{\text{IN,min}}; U_{\text{IN,max}}]$, the output voltage of the converter could be estimated by (9).

Although the control principle (Fig. 19) of the three-phase qZSI in the shoot-through (voltage boost) operating mode is more complicated, the resulting advantages of the three-phase intermediate ac link over the single-phase one are obvious:

1) lower rms current through the inverter and rectifier switches (higher power transfer through the switch with the same level of switch current and voltage stresses);

2) reduced isolated transformer's volume (and weight) due to reduced overall yoke volume and reduced voltage and magnetic stresses;

3) reduced ratings of passive components of the qZS network due to an increase by a factor of three of its operating frequency;

4) windings of isolation transformers in the three-phase isolation transformer stack, which could be connected in different configurations to obtain the desired output voltage.

Fig. 19 shows the operating principle of the three-phase qZSI in the shoot-through (voltage boost) mode. SA, SB, and SC represent the theoretical switching pattern of the traditional three-phase VSI with 120° shifted control signals. The generation principle of the shoot-through states is similar to that of the single-phase qZSI. The resulting line voltages of the primary winding of the isolation transformer during the shoot-through states are presented as U_{AB}, U_{BC}, and U_{CA}, as shown in Fig. 19. It is noticeable that, during the shoot-through, the inverter output voltage drops to zero, thus splitting the primary winding voltage waveform and reducing the operating duty cycle of the isolation transformer

$$D_A = 1 - D_S \qquad (11)$$

where D_A and D_S are the duty cycles of the active and shoot-through states, respectively.

Figs. 20 and 21 show the experimental waveforms of the proposed three-phase converter. The following system parameters were assumed for the qZSI-based converter during the experiments: $P = 500$ W, $C1 = C2 = 240$ μF, $L1 = L2 = 50$ μH, and $C3 = C4 = 10$ μF. The three-phase isolation transformer has the turns ratio of $1:1$. As shown in Fig. 20(a), the three-phase qZSI operates with continuous input current. The operating frequency of the qZS network is six times higher than the fundamental harmonic frequency of the isolation transformers.

As in the case of the single-phase VDR discussed earlier, the proposed three-phase VDR could provide output voltage without intolerable ripple and with the magnitude that is twice the amplitude voltage value of the secondary winding of the isolation transformer in all operating points of the converter (Fig. 21).

VI. CONCLUSION

This paper has presented two new isolated step-up dc/dc converter topologies with qZSIs. The topologies are intended for applications with widely varying input voltage and stabilized output voltage and when the galvanic separation of the input and output sides is required. The high-frequency transformer stack is responsible for providing the input/output galvanic isolation demanded in many applications. This paper has focused on an example of the step-up dc/dc converter with high-frequency isolation for the distributed power generation systems. The operating principle, converter design methodology, simulation, and experimental results have been presented and analyzed. Moreover, to improve the power density and reliability, the updated converter topology with the three-phase
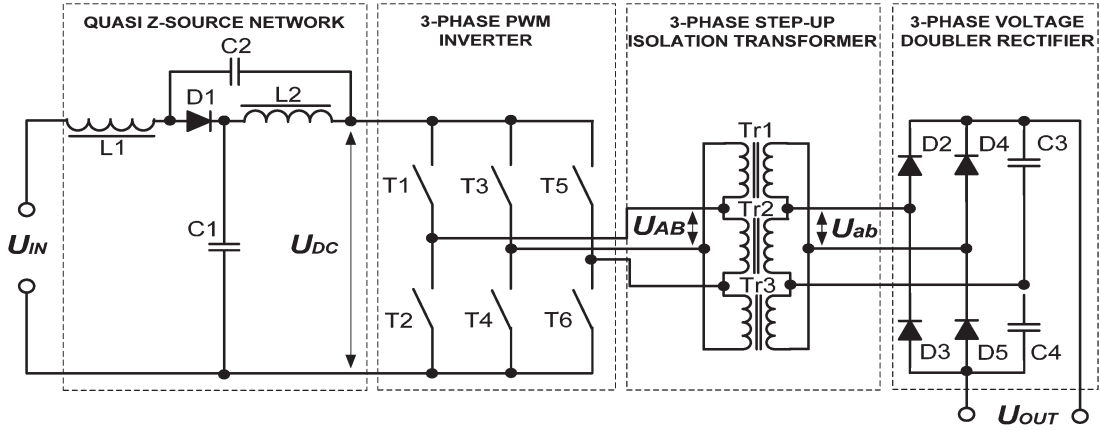
Fig. 18.   Simplified power circuit diagram of the three-phase isolated dc/dc converter with a qZS network and VDR.
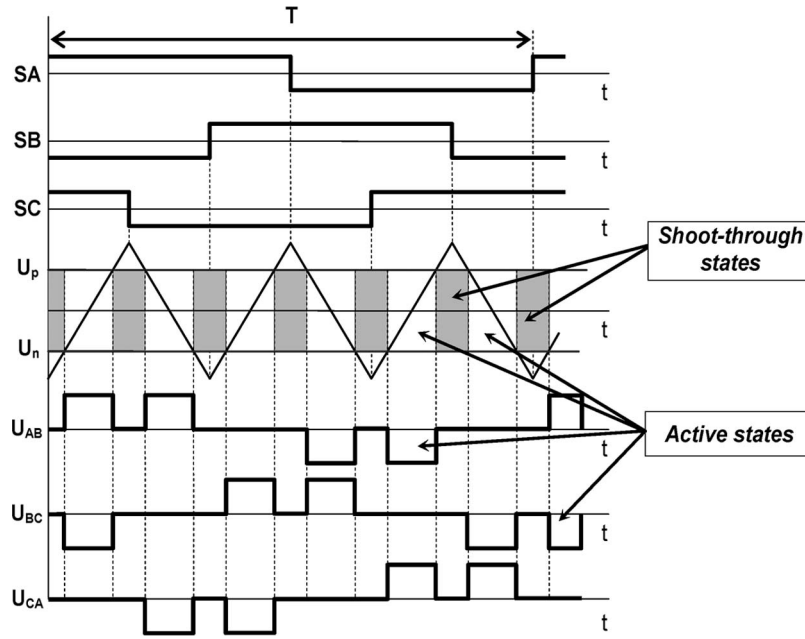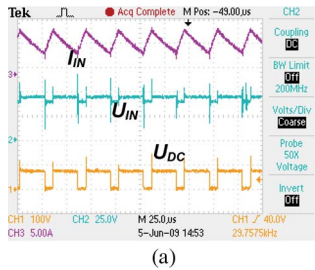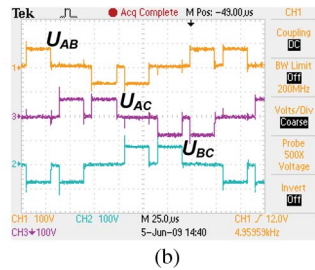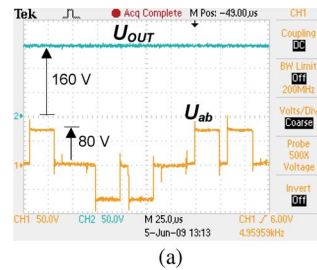

Fig. 19.   Proposed operating principle and resulting voltages of the three-phase qZSI in the shoot-through (voltage boost) mode.

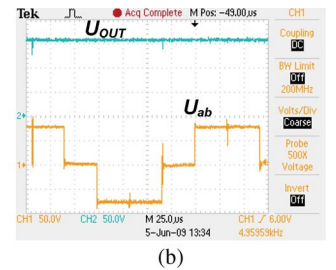Fig. 20.   Experimental waveforms of the proposed converter operating at minimal input voltage ($U_{\mathrm{IN}} = 40$ V) and maximal shoot-through duty cycle ($D_S = 0.25, D_A = 0.75$). (a) Input voltage U_{IN}, current I_{IN}, and dc-link U_{DC} voltages. (b) Line voltages ($U_{\mathrm{AB}}, U_{\mathrm{AC}}, U_{\mathrm{BC}}$) of the primary winding of the three-phase isolation transformer stack.

Fig. 21.   Experimental waveforms of the three-phase VDR at different input voltage conditions. (a) Input voltage $U_{\mathrm{IN}} = 40$ V, $D_S = 0.25$, and $D_A = 0.75$. (b) Input voltage $U_{\mathrm{IN}} = 80$ V, $D_S = 0$, and $D_A = 1$.

auxiliary ac link and the three-phase VDR was proposed and verified.

The proposed converters have the following key features in comparison to traditional topologies.

1) The qZSI implemented on the primary side of the converter could provide both the voltage boost and buck functions with no additional switches, only by use of a special control algorithm.

2) The qZSI has an excellent immunity against the cross conduction of the top- and bottom-side inverter switches. Moreover, the qZSI implemented can boost the input voltage by introducing a shoot-through operation mode, which is forbidden in traditional VSIs.

3) The qZSI implemented has the continuous input current (input current never drops to zero) during the shoot-through (voltage boost) mode.

4) The high-frequency step-up isolation transformer provides the required voltage gain as well as input–output galvanic isolation demanded in several applications.

5) The VDR implemented on the converter secondary side has the improved rectification efficiency due to the reduced voltage drop (twice reduced number of rectifying diodes and full elimination of the smoothing inductor).

6) The turns number of the secondary winding of the isolation transformer could be reduced by 62% (turns ratio of 1 : 3.75 in the case of VDR instead of 1 : 10 of traditional full-bridge rectifiers) due to the voltage doubling effect available with the VDR.

Finally, it could be stated that the proposed qZSI-based dc/dc converters with a high-frequency step-up transformer and a VDR could be positioned as a new alternative for the front-end dc/dc converter for residential power systems with the operating power up to 10 kW. Moreover, with several modifications, the proposed converters could be extended to photovoltaic and regenerative FC applications as well as to telecom, marine, and aerospace applications.

REFERENCES

[1] A. F. Zobaa and C. Cecati, "A comprehensive review on distributed power generation," in *Proc. SPEEDAM*, 2006, pp. 514–518.

[2] J. Padulles, G. W. Ault, and J. R. McDonald, "An approach to the dynamic modelling of fuel cell characteristics for distributed generation operation," in *Proc. IEEE Power Eng. Soc. Winter Meeting*, 2000, vol. 1, pp. 134–138.

[3] W. Choi, P. Enjeti, and J. W. Howze, "Fuel cell powered UPS systems: Design considerations," in *Proc. IEEE 34th PESC*, Jun. 15–19, 2003, vol. 1, pp. 385–390.

[4] M. H. Todorovic, L. Palma, and P. N. Enjeti, "Design of a wide input range DC–DC converter with a Robust power control scheme suitable for fuel cell power conversion," *IEEE Trans. Ind. Electron.*, vol. 55, no. 3, pp. 1247–1255, Mar. 2008.

[5] S. K. Mazumder, R. K. Burra, and K. Acharya, "A ripple-mitigating and energy-efficient fuel cell power-conditioning system," *IEEE Trans. Power Electron.*, vol. 22, no. 4, pp. 1437–1452, Jul. 2007.

[6] J. S. Yu and P. N. Enjeti, "A high frequency link direct dc-ac converter for residential fuel cell power systems," in *Proc. IEEE 35th PESC*, Jun. 20–25, 2004, vol. 6, pp. 4755–4761.

[7] J. C. Han and P. N. Enjeti, "A new soft switching direct converter for residential fuel cell power system," in *Conf. Rec. 39th IEEE IAS Annu. Meeting*, Oct. 3–7, 2004, vol. 2, pp. 1172–1177.

[8] S. K. Mazumder, R. Burra, R. Huang, M. Tahir, K. Acharya, G. Garcia, S. Pro, O. Rodrigues, and E. Duheric, "A high-efficiency universal grid-connected fuel-cell inverter for residential application," *IEEE Trans. Power Electron.*, 2009, to be published.

[9] G. K. Andersen, C. Klumpner, S. B. Kjaer, and F. Blaabjerg, "A new green power inverter for fuel cells," in *Proc. IEEE 33rd PESC*, 2002, vol. 2, pp. 727–733.

[10] R. Sharma and H. Gao, "A new DC-DC converter for fuel cell powered distributed residential power generation systems," in *Proc. 21st Annu. IEEE APEC*, Mar. 19–23, 2006, pp. 1014–1018.

[11] K. Sternberg and H. Gao, "A new DC/DC converter for solid oxide fuel cell powered residential systems," in *Proc. 34th IEEE IECON*, Nov. 10–13, 2008, pp. 2273–2277.

[12] W. Jin, F. Z. Peng, J. Anderson, A. Joseph, and R. Buffenbarger, "Low cost fuel cell converter system for residential power generation," *IEEE Trans. Power Electron.*, vol. 19, no. 5, pp. 1315–1322, Sep. 2004.

[13] H. Xu, L. Kong, and X. Wen, "Fuel cell power system and high power DC-DC converter," *IEEE Trans. Power Electron.*, vol. 19, no. 5, pp. 1250–1255, Sep. 2004.

[14] M. Nymand and M. Andersen, "High efficiency isolated boost DC-DC converter for high-power low-voltage fuel cell applications," in *IEEE Trans. Ind. Electron.*, Feb. 2010, vol. 57, no. 2, pp. 505–514.

[15] J. Anderson and F. Z. Peng, "Four quasi-Z-Source inverters," in *Proc. PESC*, Jun. 15–19, 2008, pp. 2743–2749.

[16] F. Z. Peng, "Z-source inverter," *IEEE Trans. Ind. Appl.*, vol. 39, no. 2, pp. 504–510, Mar./Apr. 2003.

[17] Z. J. Zhou, X. Zhang, P. Xu, and W. X. Shen, "Single-phase uninterruptible power supply based on Z-source inverter," *IEEE Trans. Ind. Electron.*, vol. 55, no. 8, pp. 2997–3004, Aug. 2008.

[18] M. Shen and F. Z. Peng, "Operation modes and characteristics of the Z-source inverter with small inductance or low power factor," *IEEE Trans. Ind. Electron.*, vol. 55, no. 1, pp. 89–96, Jan. 2008.

[19] Y. Li, J. Anderson, F. Z. Peng, and D. Liu, "Quasi-Z-source inverter for photovoltaic power generation systems," in *Proc. 24th Annual IEEE APEC*, Feb. 15–19, 2009, pp. 918–924.

[20] J.-H. Park, H.-G. Kim, E.-C. Nho, T.-W. Chun, and J. Choi, "Grid-connected PV system using a quasi-Z-source inverter," in *Proc. 24th Annu. IEEE APEC*, Feb. 15–19, 2009, pp. 925–929.

[21] Unitrode design note DN-62 R. Mammano, Switching Power Supply Topology Voltage Mode vs. Current Mode.

[22] R. Ridley, "Current mode or voltage mode," *Switching Power Mag.*, vol. 1, no. 2, pp. 4–5, Oct. 2000.

Dmitri Vinnikov (M'07) received the Dipl.Eng., M.Sc., and Dr.Sc.techn. degrees in electrical engineering from Tallinn University of Technology, Tallinn, Estonia, in 1999, 2001, and 2005, respectively.

He is currently a Senior Researcher with the Department of Electrical Drives and Power Electronics, Tallinn University of Technology. He has authored more than 100 published papers on power converter design and development and is the holder of several utility models in this application field. His research interests include switch-mode power converters, modeling and simulation of power systems, applied design of power converters and control systems, and application and development of energy storage systems.

Indrek Roasto received the B.Sc. and M.Sc. degrees in electrical engineering from Tallinn University of Technology, Tallinn, Estonia, in 2003 and 2005, respectively, where he is currently working toward the Ph.D. degree. His Ph.D. thesis is devoted to the research and development of smart control and protection systems for high-voltage high-power galvanically isolated dc/dc converters.

He is currently a Researcher with the Department of Electrical Drives and Power Electronics, Tallinn University of Technology. He has over 30 publications and owns two utility models in the field of power electronics. His research interests are in digital control of switching power converters, including modeling, design, and simulation.